Available online at www.sciencedirect.com
ScienceDirect
Ceramics International 34 (2008) 1805–1810
CERAMICS INTERNATIONAL
www.elsevier.com/locate/ceramint

Preparation, characterization and catalytic performance of $SrTi_{0.9}Li_{0.1}O_3$ ultrafine powders

Zhaobao Pang [a], Xiaoyao Tan [a,*], Ronggang Ding [b], Zi Gu [b], Shaomin Liu [b,**]

[a] School of Chemical Engineering, Shandong University of Technology, Zibo 255049, PR China
[b] The ARC Center for Functional Nanomaterials, School of Engineering, The University of Queensland, Brisbane, Qld 4072, Australia

Received 26 April 2007; received in revised form 13 May 2007; accepted 15 June 2007
Available online 17 August 2007

Abstract

$SrTi_{0.9}Li_{0.1}O_3$ ultra-fine perovskite oxide powders were prepared by the ultrasonic spray pyrolysis technique and sol–gel method, respectively. We investigated the physical properties (i.e. crystalline phase and the microstructure) of the prepared powders using XRD, PSD, SEM and TEM techniques and also evaluated the catalytic performance of the resulting powders to the oxidative coupling of methane (OCM). By adding NH_4NO_3 into the precursor solution, uniform, solid and spherical $SrTi_{0.9}Li_{0.1}O_3$ particles with a diameter of around 500 nm and the single perovskite crystal phase can be obtained at 900 °C. The resulting $SrTi_{0.9}Li_{0.1}O_3$ ultrafine power prepared by the spray pyrolysis exhibited a much better catalytic performance (higher C_2 selectivity and C_2 yield) to OCM than that prepared by the sol–gel method.

Keywords: Spray pyrolysis; Sol–gel; Perovskite oxide; Oxidative coupling of methane

1. Introduction

Some perovskite oxides such as $SrTi_{1-x}Li_xO_3$ possess good catalytic performances for methane oxidation, and thus they can be used as the anode material for direct methane solid oxide fuel cells (SOFCs) or as the catalyst for oxidative coupling of methane (OCM) [1–3]. Such composite oxide materials can be synthesized through the solid-state reaction, co-precipitation, sol–gel or the spray pyrolysis method [4–7]. Depending on the formation routes, physical properties of the oxide powders like microstructure, surface area, particle size distribution, or homogeneity of the metal ion distribution are quite different and therefore their practical performance differs accordingly. Among the powder preparation techniques, spray pyrolysis which involves the preliminary formation of minute droplets from the mixed solution containing stoichiometric metal ions and the subsequent hot pyrolysis, attracts increasingly considerable attention in the synthesis of complex materials, due to its low cost, simple and fast characteristics [8–11]. However, because of the rapid evaporation of the solvent on the surface of the droplet, hollow or dented spherical particles [12] are often produced, leading to irregular powder morphology and low utility efficiency. Later, this method was modified by the introduction of NH_3 during pyrolysis to prevent the formation of hollow particles [13,14]. However, the droplets with concentrated solution of nitrate will react with NH_3 to form a pliable continuous skin on the surface of each droplet, which is easily collapsed to form larger particles with irregular shapes. In this work, we improved this ultrasonic spray pyrolysis technology by adding NH_4NO_3 into the precursor solution as a promoter to prepare solid and ultrafine catalyst particles for methane oxidative coupling reaction. We investigated the effects of NH_4NO_3 addition on the morphology and crystal phase of the formed powders, and evaluated the catalytic performance of ultrafine $SrTi_{0.9}Li_{0.1}O_3$ particles for the OCM reaction.

2. Experimental

2.1. Sample preparation

Fifteen milliliter tetrabutyl titanate was dissolved in 50 ml of 0.1 M nitric acid. The clean layer in the beaker bottom was transferred to another vessel using a separatory funnel.

* Corresponding author. Tel.: +86 533 2313676; fax: +86 533 2313676.
** Corresponding author. Tel.: +61 7 33467514; fax: +61 7 33656074.
E-mail addresses: cestanxy@yahoo.com.cn (X. Tan), s.liu2@uq.edu.au (S. Liu).

0272-8842/$34.00
doi:10.1016/j.ceramint.2007.06.012

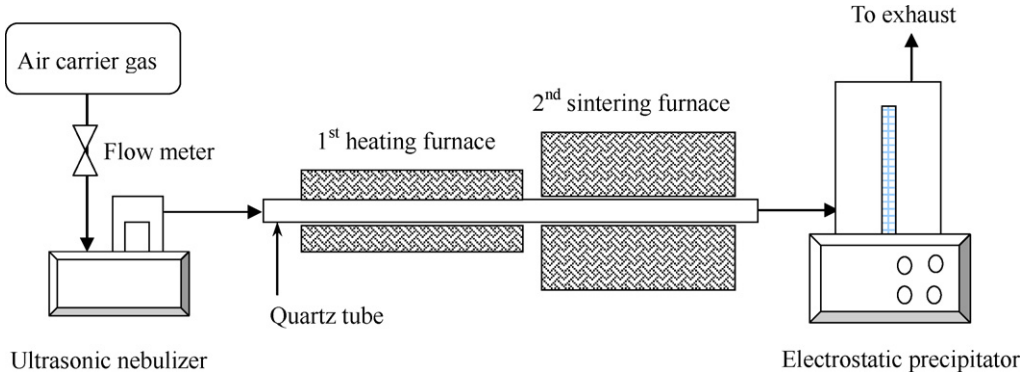

Fig. 1. Schematic diagram of the ultrasonic spray pyrolysis setup.

Stoichiometric amounts of strontium and lithium nitrates were dissolved in the above separated clean solution to get a precursor solution with the metal ion concentration of 0.2 mol/L. A certain amount of NH_4NO_3 was added into the precursor solution to a ratio of metal ion and NH_4NO_3 of 1:1. A schematic of the spray pyrolysis rig is illustrated in Fig. 1. The prepared precursor solution was injected into the ultrasonic sprayer (1.6 MHz frequency) and the air-flow rate was maintained at 0.2 m^3/h. The first temperature zone was adjusted to 300 °C to preheat the solution and remove moisture in the droplet for better pyrolysis for subsequent processes at a temperature range of 600–900 °C. The resulting particles were collected by an electrostatic collector and the exit gas was discharged into the well-ventilated fume hood.

The synthesis procedure of $SrTi_{0.9}Li_{0.1}O_3$ particles using the sol–gel method is briefly described below. The required stoichiometric amount of strontium nitrate and lithium nitrate were dissolved in the distilled water. Tetrabutyl titanate was added dropwise into the solution with certain amount of nitric acid as the chelating agent. The mixture was stirred at 70–80 °C until the transparent gel was formed. The gel was burned under continuous heating and the residues after burning were ground into powder which was heated for 2 h at 900 °C for structure characterization and catalytic performance test.

2.2. Characterization techniques

Structural phases were determined for sintered powders in a Bruker (D8 Advance) diffractometer using Cu K_a radiation. A continuous scan mode was used to collect 2θ data from 10° to 90° with a 0.02 sampling pitch and a 2°/min scan rate. X-ray tube voltage and current were set at 35 kV and 30 mA. Morphologies of the sintered samples were observed using a Scanning Electron Microscopy (FEI Sinrion 2000, Netherlands) and Transmission Electron Microscopy (HITACHI 800, Japan). A laser particle size distribution analyser (Winner 2000) was used to measure the particle size and particle size distribution of the resulting powders.

2.3. Catalytic performance test

A self-assembled quartz fixed bed reactor was used to evaluate the catalytic performance of synthesized materials. 0.5 g catalyst was loaded into the center part of the quartz reactor with a length of 25 cm and inner diameter of 0.6 cm. Both ends of the quartz tube were loaded with inert alumina spheres (200 mesh). The catalyst was activated by oxygen flow at 600 °C for 1 h before reaction. The mixture of oxygen, methane, and helium was introduced into the reactor and the flow rate was controlled by mass flow controller (D08-8B/ZM) and calibrated using a soap bubble flowmeter. The product was analyzed after 1 h of reaction. Fig. 2 illustrates the scheme of catalytic performance test.

The effluent gas composition was analyzed using a gas chromatograph (Agilent 6890N), which was equipped with a thermal conductivity detector and a 3 m-long column loaded with the carbon molecular sieve Carbosieve S-II. High purity helium (purity > 99.95%) was used as the carrier gas with a flow rate of 30 cm^3/min. The methane conversion (X_{CH_4}), C_2 selectivity (S_i) and C_2 yield (Y_{C_2}) were calculated as follows according to the gas composition before and after reaction:

$$X_{CH_4} = \left(1 - \frac{F_{out} x_{CH_4}}{F_{in} y_f}\right) \times 100\% \quad (1)$$

$$S_{C_2} = \frac{2F_{out} x_{C_2}}{F_{in} y_f - F_{out} x_{CH_4}} \times 100\% \quad (2)$$

$$Y_{C_2} = X_{CH_4} \times S_{C_2} \quad (3)$$

where y_f, x_{CH_4} are the methane contents before and after reaction, respectively. F_{in}, F_{out} are the flow rates of feed in and feed out, respectively.

3. Results and discussion

3.1. Thermal evolution to $SrTi_{0.9}Li_{0.1}O_3$ perovskite

Fig. 3 describes the X-ray diffraction patterns of $SrTi_{0.9}Li_{0.1}O_3$ powder synthesized at different conditions. Fig. 3a–d illustrates the crystal development of $SrTi_{0.9}Li_{0.1}O_3$ powder prepared from spray pyrolysis without addition of NH_4NO_3. Powders calcined at 600 and 700 °C were composed of $Sr(NO_3)_2$ and perovskite $SrTi_{0.9}Li_{0.1}O_3$. When the calcination temperature was increased to 800 and 900 °C, the XRD patterns displayed the co-existence of TiO_2 and $SrTi_{0.9}$-

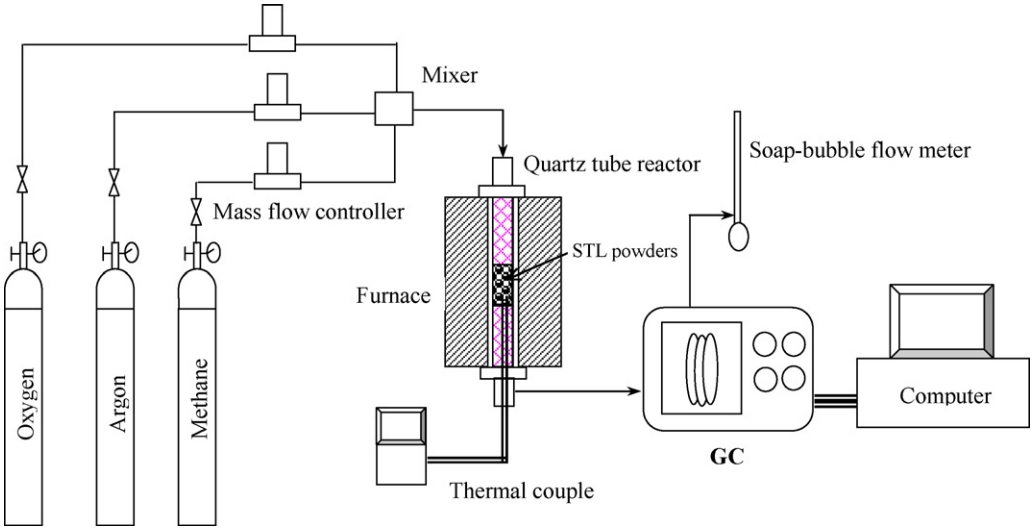

Fig. 2. Flow chart of the experimental setup for catalysis tests.

$Li_{0.1}O_3$. To transfer the crystal phase of TiO_2 oxides into the perovskite structure, a calcination temperature higher than 900 °C was needed. It is clear that when using the spray pyrolysis method without the presence of NH_4NO_3, the single perovskite crystal phase could not be easily formed, although the heat treatment temperature was up to 900 °C. By contrast, a clean and single perovskite structure (Fig. 3e) was formed for the powders prepared by the sol–gel method, where the sintering was also carried out at 900 °C.

Fig. 4 shows the XRD patterns of the $SrTi_{0.9}Li_{0.1}O_3$ particles prepared by the spay pyrolysis with NH_4NO_3 in the precursor solution at various temperatures. Noteworthy is that the TiO_2 intermediate phase was not observed in the XRD pattern of the powder prepared at 800 °C and that a single perovskite structure can be formed at 900 °C. In comparison of Figs. 3 and 4, it is clear that the addition of NH_4NO_3 is favorable to form $SrTiO_3$ perovskite crystal phase, possibly because the formation of TiO_2 intermediate phase was avoided and the burning of NH_4NO_3 in the precursor solution provide additional heat for the solution pyrolysis.

3.2. Microstructure of the particles

SEM pictures of $SrTi_{0.9}Li_{0.1}O_3$ particles synthesized by different processes are shown in Fig. 5. We can see from Fig. 5a that the $SrTi_{0.9}Li_{0.1}O_3$ powders prepared by the spray pyrolysis without NH_4NO_3 addition are composed of hollow and partially collapsed spherical particles with a wide size distribution. The morphology of the resulting particles may have resulted from the lower melting points of strontium nitrate (570 °C) and lithium nitrate (253 °C) compared to the higher operating temperature. As soon as the moisture on the surface of the droplet evaporates, the surface nitrate molts to form a compact layer which prevents further evaporation of moisture of the droplet. As a result, the rapid expansion of droplets and spraying of steam from inside the droplets gives rise to hollow, collapsed and uneven spheres. However, with the addition of NH_4NO_3 into the precursor solution, NH_3 would be produced by decomposition of NH_4NO_3 which reacts with nitrates in the droplets to rapidly form an ammonia coordination compound. At a high temperature, metal hydroxide deposition may be

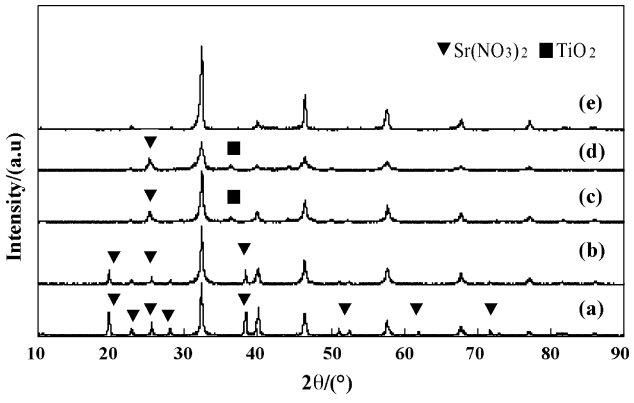

Fig. 3. XRD patterns of the particles prepared by spray pyrolysis without addition of NH_4NO_3: (a) 600 °C; (b) 700 °C; (c) 800 °C; (d) 900 °C; (e) sol–gel method followed by heat-treatment at 900 °C for 2 h.

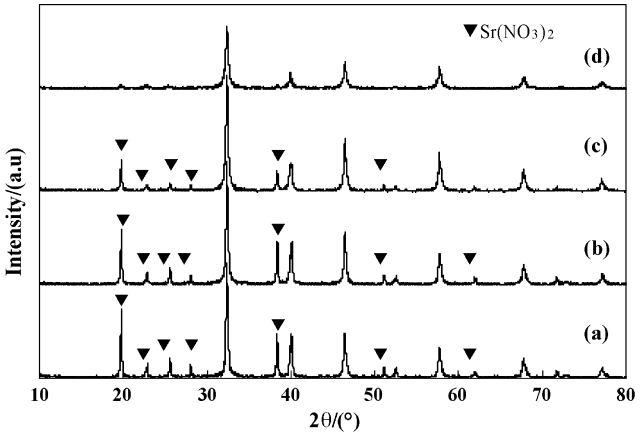

Fig. 4. XRD patterns of the particles prepared by spray pyrolysis with NH_4NO_3 in the precursor solution at various temperatures: (a) 600 °C; (b) 700 °C; (c) 800 °C; (d) 900 °C.

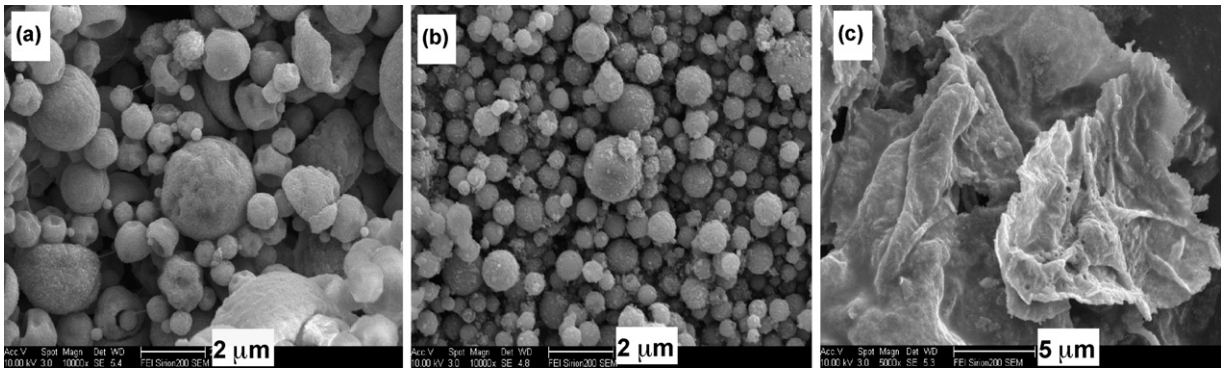

Fig. 5. SEM images of the $SrTi_{0.9}Li_{0.1}O_3$ particles prepared by: (a) S-P method at 900 °C without NH_4NO_3 in the precursor solution; (b) S-P method at 900 °C with NH_4NO_3 in the precursor solution; (c) sol–gel method.

formed from the resulting ammonia coordination compound, which makes the droplet shrink drastically and promotes the formation of solid spherical particles. Therefore, the smaller and more uniform integrated solid particles were yielded in the case that NH_4NO_3 was added as a promoter, as shown in Fig. 5b. TEM images of the $SrTi_{0.9}Li_{0.1}O_3$ particles prepared by spray pyrolysis at 900 °C with NH_4NO_3 (Fig. 6) confirms that they have a solid but not a hollow structure. By contrast, the powders produced by the sol–gel method are large particle agglomerates in a sheet structure, as shown in Fig. 5c. This is because the gel burning process is too mild to separate the product particles; subsequent mechanical grinding is necessary to get smaller particles from these sheet structures.

3.3. Particle size distribution

Fig. 7 gives the particle size distribution of the $SrTi_{0.9}Li_{0.1}O_3$ powders prepared by different methods. It should be mentioned that, without any further processing, all the samples for characterization were taken directly from the furnace when it was cooling down to room temperature. $SrTi_{0.9}Li_{0.1}O_3$ powders prepared by the spray pyrolysis possess a narrow size distribution in the range of 0.2–10 μm (Fig. 7a and b). Especially, when NH_4NO_3 was added in the precursor solution; the particles size was further decreased to 0.2–1 μm, as shown in Fig. 7b. This result agrees well with the SEM observation. Therefore, it may be concluded that the addition of NH_4NO_3 in the precursor solution is favorable to the production of $SrTi_{0.9}Li_{0.1}O_3$ perovskite powders with smaller particle size and more uniform particle size distribution. Similar phenomenon was also observed by Kang and Choi to prepare blue phosphor powder using the same technology [15]. In contrast to the method of spray pyrolysis, the particle size of $SrTi_{0.9}Li_{0.1}O_3$ prepared by sol–gel method is in a wider distribution which ranges from 0.2 to 70 μm and most of the particles have a size around 35 μm as shown in Fig. 7c.

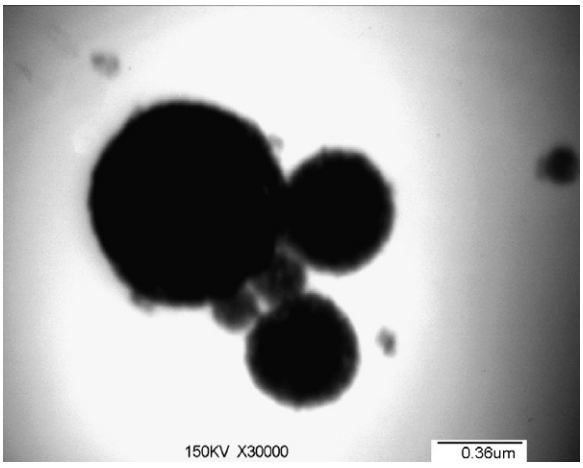

Fig. 6. TEM image of the $SrTi_{0.9}Li_{0.1}O_3$ particles prepared by S-P process at 900 °C with NH_4NO_3 in the precursor solution.

3.4. Catalytic performance test

The catalytic performance of the $SrTi_{0.9}Li_{0.1}O_3$ perovskite from sol–gel and spray pyrolysis to the OCM reaction is shown in Table 1. It can be seen that, at the operating temperatures ranging from 750 to 850 °C, $SrTi_{0.9}Li_{0.1}O_3$ perovskite oxides prepared by the two methods exhibit noticeably different C_2 selelctivities and C_2 yields but slightly different methane conversions. The powder prepared by spray pyrolysis gives much higher C_2 selelctivities or yields than the sol–gel method. For example, at 800 °C, the perovskite prepared by spray pyrolysis and sol–gel method gave C_2 selectivities of 48.69 and 4.61%, respectively. We note that the catalytic performance of $SrTi_{0.9}Li_{0.1}O_3$ particles synthesized by the sol–gel prepared method is comparable to the reported values of $SrTiO_3$ without incorporation [3]. It was generally considered that doping of Li in the B site of the $SrTiO_3$ perovksite increases the content of active oxygen species which are helpful to the OCM reaction [16]. Therefore, Li incorporated into the sol–gel produced powders actually played very little role in the enhancement of catalytic properties to the OCM. This can be explained that in the sol–gel process, lithium may be lost more easily due to the longer time of high temperature treatment at 900 °C than in the spray pyrolysis process. It is also noted that the methane conversion increases with the increase of temperature, but C_2 selectivity firstly increases and then decreases with the further increase of temperature. This can be attributed to the fact that, at high temperatures, the formed C_2 product is easily deeply oxidized to CO_2 thus lowering the C_2 selectivity.

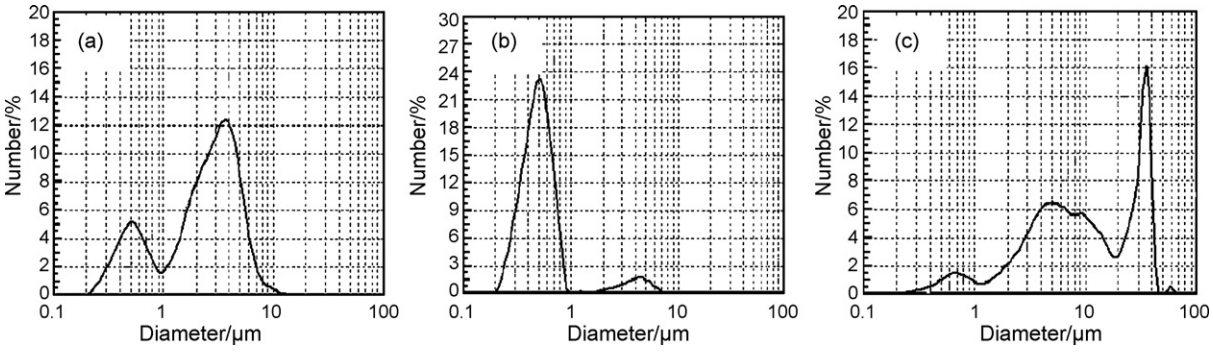

Fig. 7. Particle size distribution of $SrTi_{0.9}Li_{0.1}O_3$ powders prepared by: (a) S-P method at 900 °C without NH_4NO_3 in the precursor solution; (b) S-P method at 900 °C with NH_4NO_3 in the precursor solution; and (c) sol–gel method.

Table 1
Catalytic properties to OCM of the $SrTi_{0.9}Li_{0.1}O_3$ powders prepared by different methods (Feed flow rate: $F_{CH_4} : F_{O_2} : F_{He} = 16 : 6 : 16$ ml/min, respectively)

Method	Temperature (°C)	CH_4 conversion (%)	C_2 selectivity (%)	C_2 yield (%)
Sol–gel	750	21.59	3.36	0.73
	800	31.68	4.61	1.46
	850	32.95	3.46	1.14
Spray pyrolysis	750	27.67	27.36	7.58
	800	26.89	48.69	13.09
	850	43.18	25.65	11.08

Table 2
Catalytic performances of the $SrTi_{0.9}Li_{0.1}O_3$ powders (by spray pyrolysis) at different CH_4/O_2 feed ratios (temperature = 800 °C)

$F_{CH_4} : F_{O_2} : F_{He}$ (ml/min)	CH_4 conversion (%)	Selectivity (%)			C_2 yield (%)
		CO_x	C_2H_4	C_2H_6	
16:4:16	19.50	48.73	10.97	40.30	10
16:6:16	26.89	51.31	13.49	35.20	13.09
16:8:16	42.70	70.85	13.75	15.40	12.45

Table 2 reports the activity and selectivity of the $SrTi_{0.9}Li_{0.1}O_3$ perovskite oxide powders synthesized by spray pyrolysis at different feed ratios where the temperature is kept at 800 °C. It is obvious that with the decline of CH_4/O_2 ratios, methane conversion rapidly increased, but the selectivity of C_2H_6 noticeably decreased, while CO_x improved to some extent. These features are consistent with the general characteristics of the methane coupling reaction [3]. Both the selectivity of C_2H_4 and the C_2 content in the products are increased. This is possibly due to higher oxygen concentration in the gaseous phase which enhances the content of oxygen species adsorbed on the surface of the powders and further dehydrogenates the intermediate constituent like methyl radical.

4. Conclusions

$SrTi_{0.9}Li_{0.1}O_3$ perovskite oxide has been synthesized by the ultrasonic spray pyrolysis with strontium nitrate, lithium nitrate and tetrabutyl titanate as the parent materials. By adding NH_4NO_3 into the precursor solution, uniform, solid and spherical $SrTi_{0.9}Li_{0.1}O_3$ particles, with a diameter of around 500nm, and the single perovskite crystal phase can be achieved at 900 °C. The resulting $SrTi_{0.9}Li_{0.1}O_3$ ultrafine powders from the spray pyrolysis method exhibited higher C_2 selectivity and C_2 yield in methane oxidation reaction than the powders produced by the sol–gel method.

Acknowledgements

The authors gratefully acknowledge the research funding provided by the National Natural Science Foundation of China (NNSFC, No. 2067603). Liu is particularly thankful for the financial support of UQ Early Career Research Grants Scheme 2006001832.

References

[1] J. Pena-Martinez, D. Marrero-Lopez, J.C. Ruiz-Morales, Fuel cell studies of perovskite-type materials for IT-SOFC, J. Power Sources 159 (2006) 914–921.
[2] W. Yang, Q. Yan, X. Fu, Oxidative coupling of methane over Sr-Ti, Sr-Sn perovskites and corresponding layered perovskites, React. Kinet. Catal. L. 54 (1995) 21–27.
[3] J. Miao, Y. Fan, Y. Jin, A study on catalytic properties of perovskite-type oxide $SrTiO_3$ catalysts for oxidative coupling of methane, Chin. J. Inorg. Chem. 20 (2004) 967–970.
[4] A. Aatiq, Synthesis and crystal structure of the new perovskite $CaLa_2CaTi_2O_9$ (= $(Ca_{1/3}La_{2/3})_A(Ca_{1/3}Ti_{2/3})_BO_3$), Solid State Sci. 5 (2003) 745–749.
[5] U. Chellam, Z.P. Xu, H.C. Zeng, Low-temperature synthesis of $Mg_xCo_{1-x}Co_2O_4$ spinel catalysts for N_2O decomposition, Chem. Mater. 12 (2000) 650–658.
[6] L. Ji, J. Lin, K.L. Tan, H.C. Zeng, Synthesis of high-surface-area alumina using aluminum tri-sec-butoxide-2,4-pentanedione-2-propanol-nitric acid precursors, Chem. Mater. 12 (2000) 931–939.

[7] S. Liu, X. Tan, K. Li, R. Hughes, Synthesis of strontium cerates-based perovskite ceramics via water-soluble complex precursor routes, Ceram. Int. 28 (2002) 327–335.
[8] V.V. Pankov, Synthesis of $BaFe_{12}O_{19}$ powder by modified coprecipitation and spray pyrolysis methods, Inorg. Mater. 40 (2004) 979–984.
[9] K.C. Hiso, S.C. Liao, Y.J. Che, Synthesis, characterization and photocatalytic property of nanostructured Al-doped ZnO powders prepared by spray pyrolysis, Mater. Sci. Eng. A 447 (2007) 71–76.
[10] S.C. Tsai, Y.L. Song, C.S. Tsai, C.C. Yang, W.Y. Chiu, H.M. Lin, Ultrasonic spray pyrolysis for nanoparticles synthesis, J. Mater. Sci. 39 (2004) 3647–3657.
[11] H.B. Su, D.O. Welch, The effects of space charge, dopants, and strain fields on surfaces and grain boundaries in YBCO compounds, Supercond. Sci. Technol. 18 (2005) 24–34.
[12] N. Kieda, G.L. Messing, Microfoamy particles of copper oxide and nitride by spray pyrolysis of copper–ammine complex solution, J. Mater. Sci. Lett. 17 (1998) 299–301.
[13] S. Che, K. Takada, Formation of spherical dense nickel particles by pyrolyzing the aerosol of an ammine complex solution in nitrogen atmosphere, J. Mater. Sci. Lett. 17 (1998) 1227–1230.
[14] H.F. Yu, A.M. Gadalla, Preparation of $NiFe_2O_4$ powder by spray pyrolysis of nitrate aerosols in NH_3, J. Mater. Res. 11 (1996) 663–670.
[15] M.J. Kang, S.Y. Choi, Preparation of Sr_2CeO_4 blue phosphor by ultrasonic spray pyrolysis: effect of NH_4NO_3 addition, J. Mater. Sci. 37 (2002) 2721–2729.
[16] C.Y. Yu, W.Z. Li, G.A. Martin, C. Mirodatos, Studies of $CaTiO_3$ based catalysts for the oxidative coupling of methane, Appl. Catal. A: Gen. 158 (1997) 201–214.